Networks and Heterogeneous Media

https://www.aimspress.com/journal/nhm

NHM, 20(1): 52–64.
DOI: 10.3934/nhm.2025004
Received: 31 October 2024
Revised: 26 December 2024
Accepted: 06 January 2025
Published: 10 January 2025

Research article

Anti-plane interfacial waves in a square lattice

Victor A. Eremeyev*

Department of Civil and Environmental Engineering and Architecture (DICAAR), University of Cagliari, Via Marengo 2, Cagliari 09-123, CA, Italy

* **Correspondence:** Email: eremeyev.victor@gmail.com; Tel: +390706755417; Fax: +390706755418.

Abstract: Using the lattice dynamics approach, we discussed the propagation of interfacial waves localized near the interface in an infinite square lattice. The interface has been modeled as a single-particle layer of material particles with masses and elastic bonds different from those in the bulk. In this lattice structure there were anti-plane interface waves, i.e., waves that decayed exponentially with distance from the interface. Such waves could be useful for determining material properties in the vicinity of the interface. We obtained equations of motion and analyzed the corresponding dispersion relations for steady-state solutions. Here, the dispersion equation related the circular frequency to the wave number. In addition, we provided a comparison of the dispersion relations with those derived within the Gurtin-Murdoch surface elasticity. To do this, we have used the scaling law that links the continuum and discrete models. Unlike the continuum model, in the discrete model the wave number was limited by the first Brillouin zone, whereas in the continuum model it took a range from zero to infinity. The detailed parametric analysis was given for the discrete model. Finally, other models of interfaces in the case of a square lattice were discussed.

Keywords: surface elasticity; lattice dynamics; interfacial waves; square lattice; anti-plane motions

1. Introduction

Originating from earlier work by Laplace, Young, and Gibbs [1–4], surface elasticity is an example of an extended continuum model that has recently found several applications in small scale material modeling, see, for example, [5–8]. Within this approach, called Gurtin-Murdoch surface elasticity, in addition to the constitutive relations in the bulk, a surface strain energy and a surface kinetic energy are introduced [9, 10]. As a result, there are surface stresses which generalize those known from the theory of capillary surface tension. Obviously, the surface energetics essentially influence the propagation of surface waves, including anti-plane surface/interface waves; see [11–16] and references therein. Recently, such wave analysis has been proposed for the experimental determination of surface elastic

parameters in [17, 18]. More general models of surface elasticity can be found in the literature, such as the Steigmann-Ogden surface elasticity [19, 20] and even more general; see [21, 22].

Of course, surface stresses can be explained by classical molecular considerations; see, for example, [23] or [24]. Moreover, considering a square lattice, some correspondence between Gurtin-Murdoch elasticity and lattice dynamics has been demonstrated in [25, 26].

The aim of this paper is to extend the results of [25, 26] toward interfacial waves. Here we again consider an infinite square lattice of the same particles except for one row where the material particles have different mass and the bond stiffness. This series of different particles can be treated as an interfacial layer. In the vicinity of this layer, under certain conditions, there are possible anti-plane waves. For this type of wave we derive the dispersion relations. It should be noted that dispersion is an important characteristic of wave propagation [27, 28]. In particular, dispersion data can be used to validate the continuum or discrete model used and to determine material parameters; see, for example, [29–33] for microstructured media.

The remainder of the paper is organized as follows. In Section 2, we present the statement of the problem using both lattice dynamics and Gurtin-Murdoch surface elasticity. Dispersion relations are presented in Section 3. Finally, in Section 4, we also discuss the correspondence between these two models and the related scaling law.

2. Statement of the problem

In the following we discuss anti-plane waves localized in the vicinity of a straight material interface which separates two elastic half-spaces. Material properties of the half-spaces are different, in general. We consider two models, discrete and continuum. As a discrete model we use a square lattice, whereas as a continuum model model we apply the classic elastic of isotropic solids. Both models are illustrated in Figure 1a) and b). Within these models we have almost the same kinematics. Note that the square lattice corresponds to cubic symmetry. Moreover, such a geometry generally refers to a 3D lattice with 3D cells in the form of a rectangular cuboid. So, the corresponding continuum model should have the same symmetry. On the other hand, in the case of anti-plane deformations, cubic and isotropic materials give the same equations. In the lattice, the position of a material particle is given as a function of discrete lattice coordinates [23, 34, 35]

$$\mathbf{r} = xa\mathbf{i}_1 + ya\mathbf{i}_2 + za\mathbf{i}_3 + u\mathbf{i}_3, \quad u = u(x, y, t),$$

where x, y, z are integers, t is time, $\mathbf{i}_1$, $\mathbf{i}_2$, $\mathbf{i}_3$ are the unit base vector related to the Cartesian coordinates x, y, z, and a is the lattice cell size; see Figure 1.

Instead, in the continuum model the position-vector of a material particle has the form

$$\mathbf{r} = x\mathbf{i}_1 + y\mathbf{i}_2 + z\mathbf{i}_3 + u\mathbf{i}_3, \quad u = u(x, y, t),$$

where x, y, z are real numbers, in general.

Note that for simplicity, we keep the same notations for a lattice coordinate and for continuum coordinates.

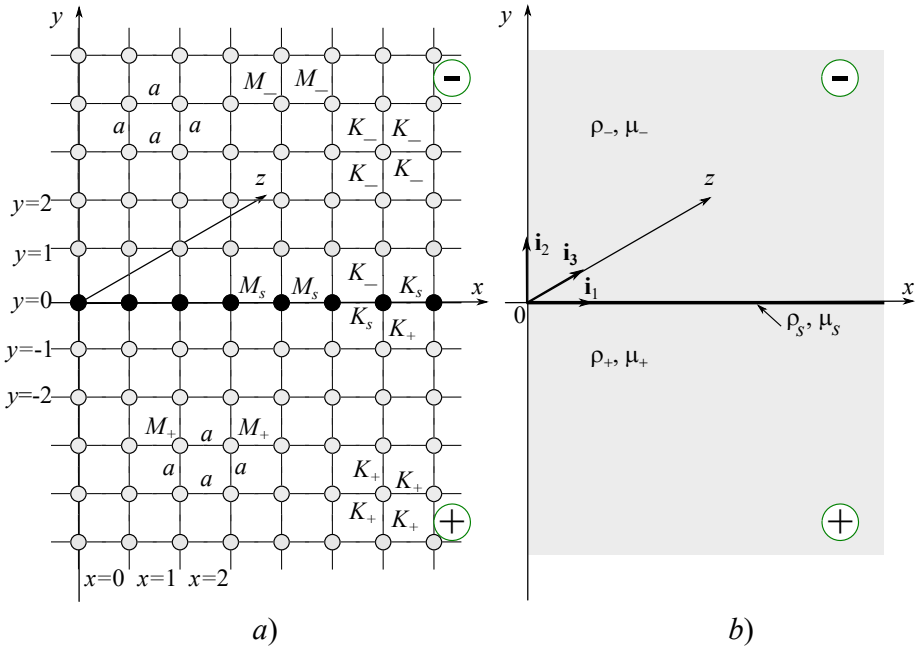

Figure 1. Two models of material interface: a) square lattice, b) elastic space.

2.1. Lattice dynamics

Let us consider a square lattice in more detail. Let $M_\pm$ and $K_\pm$ be the masses of the particles and the stiffness of the elastic bonds between them in the corresponding half-space $\pm y > 0$. As a material interface, we introduce a set of material particles of mass M_s connected by an elastic bond of stiffness K_s. We also assume that the interface particles are connected to the particles in the bulk by bonds of stiffness $K_\pm$.

As a result, we have equations of motion in the bulk

$$M_\pm \ddot{u}_\pm(x,y,t) = K_\pm \left[u_\pm(x+1,y,t) + u_\pm(x-1,y,t) + u_\pm(x,y-1,t) + u_\pm(x,y+1) - 4u_\pm(x,y,t)\right], \quad (2.1)$$

see, e.g., [25, 35]. For the surface $y = 0$, we have a different equation of motion given by

$$\begin{aligned} M_s \ddot{u}(x,0,t) =& K_s \left[u_+(x+1,0,t) + u_+(x-1,0,t) - 2u(x,0,t)\right] \\ &+ K_+ \left[u_+(x,-1,t) - u_+(x,0,t)\right] + K_- \left[u_-(x,+1,t) - u(x,0,t)\right]. \end{aligned} \quad (2.2)$$

Note that here u_+ and u_- are defined in the half-spaces $y < 0$ and $y > 0$, respectively, where u refers to $y = 0$.

We are looking for a solution in the form

$$u_\pm = U \exp(\mathrm{i}\xi x - \mathrm{i}\omega t) \exp(\pm\eta_\pm y), \quad u = U \exp(\mathrm{i}\xi x - \mathrm{i}\omega t), \quad (2.3)$$

where ξ is a wave number, ω is a circular frequency, U is an amplitude, $\mathrm{i} = \sqrt{-1}$ is the imaginary unit, and $\eta_\pm$ is assumed to be positive.

Substituting Eq (2.3) into Eqs (2.1) and (2.2), we obtain the equations

$$-M_+\omega^2 = K_+ \left[2\cos\xi + 2\cosh\eta_+ - 4\right], \quad (2.4)$$

$$-M_-\omega^2 = K_-\left[2\cos\xi + 2\cosh\eta_- - 4\right], \tag{2.5}$$

$$-M_s\omega^2 = K_s\left[2\cos\xi - 2\right] + K_+\left[e^{-\eta_+} - 1\right] + K_-\left[e^{-\eta_-} - 1\right], \tag{2.6}$$

which play a role of dispersion relations.

2.2. *Gurtin–Murdoch surface elasticity*

Following [14], let us briefly introduce the basic equations within the linear Gurtin–Murdoch surface elasticity. Considering only anti-plane motions, we have the wave equations in the bulk

$$\mu_\pm \Delta u_\pm = \rho_\pm \ddot{u}_\pm, \quad \Delta = \frac{\partial^2}{\partial x^2} + \frac{\partial^2}{\partial y^2}, \tag{2.7}$$

where $\mu_\pm$ are the shear moduli, $\rho_\pm$ are the mass densities, and $u_\pm = u_\pm(x, y, t)$ are the displacements in z-direction, all defined in the corresponding half-spaces $\mp y \geq 0$; see Figure 1b).

At the interface $y = 0$ we have the following compatibility conditions:

$$\mu_+ \frac{\partial u_+}{\partial y} - \mu_- \frac{\partial u_-}{\partial y} = \mu_s \frac{\partial^2 u}{\partial x^2} - \rho_s \ddot{u}_\pm, \quad u_+ = u_- \equiv u, \tag{2.8}$$

where μ_s is the surface shear modulus and ρ_s is the surface mass density. Eq (2.8) expresses the balance of forces and the continuity of displacements across the interface, i.e., they describe the perfect contact. For non-perfect contact, we refer to [14].

Note that Eqs (2.7) and (2.8) are straightforward counterparts of the discrete equations of motion Eqs (2.1) and (2.2), respectively.

Let us consider solutions of the form

$$u_\pm = U_\pm \exp\left[\mathrm{i}(kx - \omega t)\right] \exp\left(\pm\kappa_\pm y\right), \tag{2.9}$$

where $U_\pm$ are the constant amplitudes, k is the wave number, and $\kappa_\pm$ are given by [14]

$$\kappa_\pm = \sqrt{k^2 - \frac{\omega^2}{c_{T\pm}^2}}, \quad c_{T\pm} = \sqrt{\frac{\mu_\pm}{\rho_\pm}},$$

where $c_{T\pm}$ is the shear wave velocity in the corresponding half-space. Note that the functions defined by Eq (2.9) decay exponentially with distance from the interface if both $\kappa_\pm$ are real. This gives us the constraint on the phase velocity $c = \omega/k$:

$$c < \min\left(c_{T+}, c_{T-}\right).$$

Substituting Eq (2.9) into Eq (2.8), we came to the dispersion equation relating ω and k

$$\mu_+ \sqrt{k^2 - \frac{\omega^2}{c_{T_+}^2}} + \mu_- \sqrt{k^2 - \frac{\omega^2}{c_{T_-}^2}} = \rho_s \omega^2 - \mu_s k^2. \tag{2.10}$$

Eq (2.10) could be solved with respect to k as follows:

$$|k| = \frac{\sqrt{1 - \frac{c^2}{c_{T_+}^2}} + \frac{\mu_-}{\mu_+}\sqrt{1 - \frac{c^2}{c_{T_-}^2}}}{\frac{\mu_s}{\mu_+}\left(\frac{c^2}{c_s^2} - 1\right)}, \tag{2.11}$$

where $c_s = \sqrt{\mu_s/\rho_s}$. From Eq (2.11), it also follows that $c > c_s$.

3. Dispersion curves

Let us analyze the dispersion relations Eqs (2.4)–(2.6) and (2.11) in more detail.

3.1. Gurtin–Murdoch surface elasticity

First, let us discuss the continuum model, i.e., Eq (2.11). We begin from the symmetric case, i.e., when $\mu_\pm = \mu$, $\rho_\pm = \rho$. In this case, Eq (2.11) takes the form

$$|k| = 2\,\frac{\mu}{\mu_s}\,\frac{\sqrt{1-\frac{c^2}{c_T^2}}}{\left(\frac{c^2}{c_s^2}-1\right)}. \tag{3.1}$$

In the Gurtin–Murdoch surface elasticity, there are two length-scale parameters, dynamic and static, defined as follows:

$$\ell_{st} = \frac{\mu_s}{\mu}, \quad \ell_{dyn} = \frac{\rho_s}{\rho}.$$

Using the latter, we can rewrite Eq (3.1) in dimensionless form as follows:

$$|k|\ell_{st} = 2\,\frac{\sqrt{1-\overline{c}^2}}{\frac{\ell_{dyn}}{\ell_{st}}\,\overline{c}^2-1}, \tag{3.2}$$

where $\overline{c} = \frac{c}{c_T}$. Obviously, Eq (3.2) has a real solution only if two inequalities are fulfilled

$$\sqrt{\frac{\ell_{st}}{\ell_{dyn}}} < \overline{c} \le 1,$$

or if $c_s < c \le c_T$. Eq (3.2) corresponds to a dispersion curve starting at point $(0, c_T)$ with the horizontal tangent and having the horizontal asymptote $c = c_s$ as $k \to \infty$.

Similarly, for the nonsymmetric case, we get the following dimensionless dispersion equation:

$$|k|\ell_{st}^{+} = \frac{\sqrt{1-\overline{c}^2} + \kappa\sqrt{1-\left(\frac{c_T^+}{c_T^-}\right)^2\overline{c}^2}}{\frac{\ell_{dyn}^+}{\ell_{st}^+}\,\overline{c}^2-1}, \tag{3.3}$$

where now $\overline{c} = \frac{c}{c_T^+}$, $\ell_{st}^+ = \frac{\mu_s}{\mu_+}$, $\ell_{dyn}^+ = \frac{\rho_s}{\rho_+}$, and $\kappa = \frac{\mu_-}{\mu_+}$. In this case, we have real solutions only if $c_s < c \le \min(c_T^-, c_T^+)$.

Dispersion curves are given in Figure 2. Here, $\overline{k} = |k|\ell_{st}^+$, and curves 1, 2, 3 correspond to the values of $\kappa = 0.8,\ 0.5,\ 0.2$, respectively. For simplicity, we assume here that $\rho_+ = \rho_-$. Upper dashed curve corresponds to the symmetric case $\mu_+ = \mu_-$, whereas the lower dashed curve relates to the absence of the half-space $y > 0$, so $\mu_- = 0$. Note that if $\mu_+ \neq \mu_-$ and $\mu_- > 0$, dispersion curves do not start at $k = 0$ as in [15, 36].

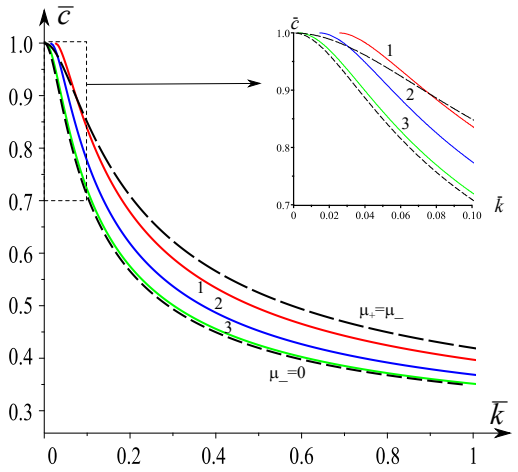

Figure 2. Dispersion curves within the Gurtin–Murdoch surface elasticity.

3.2. Lattice dynamics

We transform Eqs (2.4) and (2.5) into the following equations:

$$-\omega^2 = \frac{C_{T+}^2}{a^2}\left[2\cos\xi + 2\cosh\eta_+ - 4\right], \tag{3.4}$$

$$-\omega^2 = \frac{C_{T-}^2}{a^2}\left[2\cos\xi + 2\cosh\eta_- - 4\right], \tag{3.5}$$

whereas Eq (2.6) became

$$-\omega^2 = \frac{C_s^2}{a^2}\left[2\cos\xi - 2\right] + \frac{C_{T+}^2}{ma^2}\left[e^{-\eta_+} - 1\right] + \frac{C_{T-}^2}{ma^2}\left[e^{-\eta_-} - 1\right], \tag{3.6}$$

where $C_{T\pm} = a\sqrt{K_\pm/M_\pm}$, $C_s = a\sqrt{K_s/M_s}$, $m = M_s/M_+$.

In the following, for simplicity, we consider a symmetric case, i.e., when $K_\pm = K$ and $M_\pm = M$. Now, we have

$$-\omega^2 = \frac{C_T^2}{a^2}\left[2\cos\xi + 2\cosh\eta - 4\right], \tag{3.7}$$

$$-\omega^2 = 2\frac{C_s^2}{a^2}\left[\cos\xi - 1\right] + 2\frac{C_T^2}{ma^2}\left[e^{-\eta} - 1\right]. \tag{3.8}$$

Eqs (3.7) and (3.8) form a dispersion relation in a parametric form. The corresponding dispersion relations are shown in Figure 3. Here, $\tilde{\omega} = a\omega/C_T$ and $\chi = C_s/C_T$. Let us note that for an infinite homogeneous square lattice, the passing band is given by the relation [23]

$$\omega^2 = \frac{C_T^2}{a^2}\left[4 - 2\cos\xi - 2\cos\eta\right], \quad 0 \le \eta \le \pi. \tag{3.9}$$

It is shown in Figure 3 as a light green area bounded by dashed curves. In contrast to the Gurtin-Murdoch model, here the anti-plane motions exist in both cases $C_s < C_T$ and $C_s > C_T$. Furthermore,

when $C_s = C_T$, the associated dispersion curve coincides with the lower limit of the passing band. The solid curves correspond to $C_s < C_T$, whereas long-dash curves relate to $C_s > C_T$.

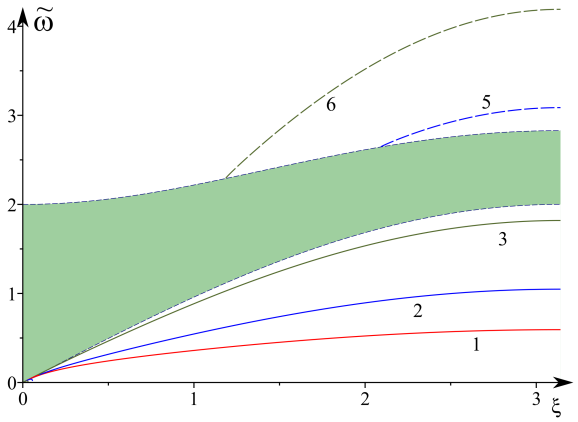

Figure 3. Dispersion curves for lattice dynamics. Here, $m = 16$, and curves 1, 2, 3, 4, 5, and 6 correspond to the following values of χ=0.25, 0.5, 0.9, 1.2, 1.5, 2, respectively. Note that curve 4 is out of the scale of the figure.

It is interesting to note that when $C_s > C_T$, the corresponding dispersion curves may consist of two parts lying outside the pass band; see curves 5 and 6 as only one part of the latter. The first parts are shown in Figure 4 for small ξ. Such a behavior depends on m. For relatively small m, the dispersion curves are given in Figure 5 for the same values of χ. So, it can be concluded that the lattice dynamics has a more complex dispersion behavior than the Gurtin-Murdoch surface elasticity, in general.

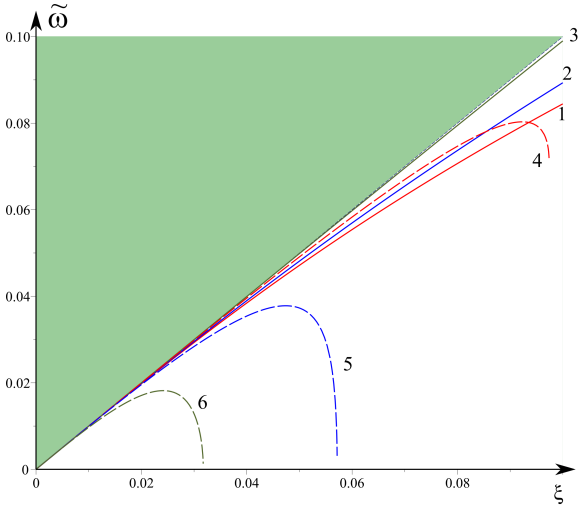

Figure 4. Dispersion curves for lattice dynamics for small ξ. Here, $m = 16$, and curves 1, 2, 3, 4, 5, and 6 correspond to the following values of χ=0.25, 0.5, 0.9, 1.2, 1.5, 2, respectively.

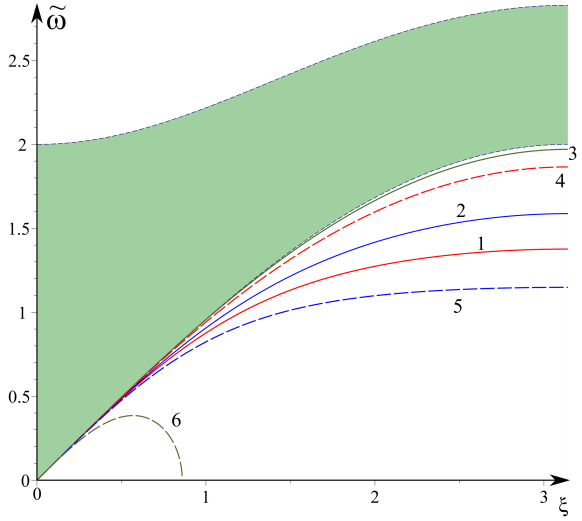

Figure 5. Dispersion curves for lattice dynamics. Here, $m = 0.9$, and curves 1, 2, 3, 4, 5, and 6 correspond to the following values of χ=0.25, 0.5, 0.9, 1.2, 1.5, 2, respectively.

4. Comparison of the models and the scaling law

Let us provide a comparison of the dispersion relations obtained within the surface elasticity and square lattice dynamics. First, we transform Eq (3.2) into the dimensionless form

$$\overline{k} = 2\frac{\sqrt{1-\frac{\overline{\omega}^2}{\overline{k}^2}}}{\left(\frac{\ell_{dyn}}{\ell_{st}}\right)^2\frac{\overline{\omega}^2}{\overline{k}^2}-1}, \tag{4.1}$$

which gives the dispersion relation in the implicit form. Similarly, the dimensionless form of Eqs (3.7) and (3.8) is given by

$$-\tilde{\omega}^2 = [2\cos\xi + 2\cosh\eta - 4], \tag{4.2}$$

$$-\tilde{\omega}^2 = 2\frac{C_s^2}{C_T^2}[\cos\xi - 1] + \frac{2}{m}[e^{-\eta} - 1]. \tag{4.3}$$

Note that k takes values from 0 to ∞, whereas ξ is in the range $[0, \pi]$. As in [25], we assume that $k = \xi/a$, so $\overline{k} = \xi l_{st}/a$ and $k \to \infty$ as $a \to 0$, i.e., in the continuum limit.

Motivated by the continuum context, we assume the following correspondence between the lattice and continuum parameters [34, 35]:

$$M = \rho a^3, \quad K = \mu a. \tag{4.4}$$

As a result, we get $c_T = C_T$.

For further comparison of the lattice dynamics and the Gurtin–Murdoch surface elasticity, we have to establish relations between M_s and ρ_s, K_s and μ_s, and between the length scale parameters ℓ_{st} and ℓ_{dyn} and the lattice cell size a. Following the scaling law proposed in [25], one can use the following scaling at $a \to 0$:

$$M_s \sim \rho_s a^2, \quad K_s \sim \mu_s. \tag{4.5}$$

In Figures 6 and 7, we demonstrate the correspondence between both theories. Here, we assume that $c_s = 0.5c_T$. Curves 1, 2, and 3 relate to ℓ_{st} equal to $0.5a,\ a,\ 2a,\ 10a$, respectively. The dashed curve relates to the lattice model model with $C_s = c_s$ and $m = 0.9$. In Figure 7, the phase velocity is given for the same parameters.

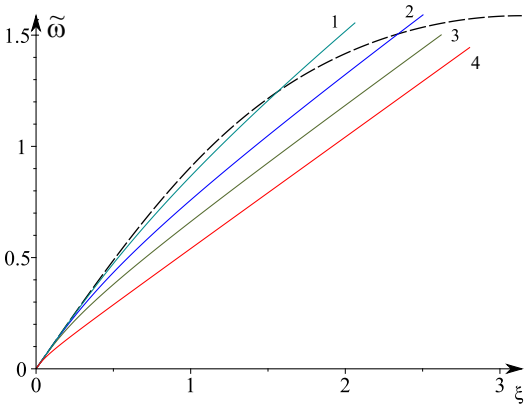

Figure 6. Dispersion curves for both theories. Dashed curve relates to the lattice model with $C_s = c_s$ and $m = 0.9$. Here, $c_s = 0.5c_T$, and curves 1, 2, 3, and 4 relate to ℓ_{st} equal to $0.5a,\ a,\ 2a,\ 10a$, respectively.

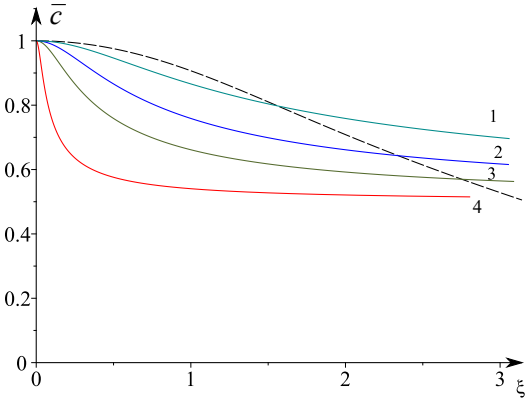

Figure 7. Phase velocities for both theories. All parameters as in Figure 6.

5. Conclusions

Considering anti-plane motions of an infinite square lattice with an interface, we have provided the detailed analysis of propagation of so-called interfacial waves, i.e., waves localised near the interface and exponentially decaying with the distance from the interface. We obtained and analysed the corresponding dispersion relations. Moreover, we provided the comparison between the Gurtin-Murdoch elasticity and lattice dynamics considering a scaling law. It has been shown that in some cases, the lattice dynamics leads to a more complex picture of the dispersion relations.

Let us note that here we restrict ourselves by possibly the simplest discrete model of interface. Indeed,

we assumed here local (pair-wise) interactions between material particles, mono-particle interface, and the symmetry in the transverse direction. As further steps, one consider more complex interface models consisting of a few rows or particles, and/or with long-range (nonlocal) interactions, as well as half-spaces of different properties. In such a case the possible dynamics could be more complex. Indeed, in the literature we can easily find more complex models of interfaces; see e.g., [37–39] for discrete and [40–42] for continuum models including micromorphic and strain gradient ones [43–45], and other results on waves in microstructured media and structures [46–49]. For example, dispersion relations for anti-plane waves in an elastic half-space with microstructured coating [50] correspond to the more general model of surface elasticity introduced in [21].

Use of AI tools declaration

The author declares that he has not used Artificial Intelligence (AI) tools in the creation of this article.

Acknowledgments

The author acknowledges the support within the project "Metamaterials design and synthesis with applications to infrastructure engineering" funded by the MUR Progetti di Ricerca di Rilevante Interesse Nazionale (PRIN) Bando 2022 - grant 20228CPHN5, Italy, and the support of the European Union's Horizon 2020 research and innovation program under the RISE MSCA EffectFact Project agreement No. 101008140.

Conflict of interest

The authors declare there is no conflict of interest.

References

1. P. S. Laplace, Sur l'action capillaire, *Supplément au livre X du Traité de mécanique céleste*, Gauthier–Villars et fils, Paris, **4** (1805), 771–777.
2. P. S. Laplace, Supplément à la théorie de l'action capillaire, *Traité de mécanique céleste*, Gauthier–Villars et fils, Paris, **4** (1806), 909–945.
3. T. Young, An essay on the cohesion of fluids, *Philos. Trans. R. Soc. London*, **95** (1805), 65–87. https://doi.org/10.1098/rstl.1805.0005
4. J. Willard Gibbs, *The Collected Works, in Thermodynamics*, Longmans, Green, New York, **1** (1928), 320.
5. H. L. Duan, J. Wang, B. L. Karihaloo, Theory of elasticity at the nanoscale, *Adv. Appl. Mech.*, **42** (2008), 1–68. https://doi.org/10.1016/S0065-2156(08)00001-X
6. J. Wang, Z. Huang, H. Duan, S. Yu, X. Feng, G. Wang, et al., Surface stress effect in mechanics of nanostructured materials, *Acta Mech. Solida Sin.*, **24** (2011), 52–82. https://doi.org/10.1016/S0894-9166(11)60009-8

7. V. A. Eremeyev, On effective properties of materials at the nano- and microscales considering surface effects, *Acta Mech.*, **227** (2016), 29–42. https://doi.org/10.1007/s00707-015-1427-y
8. S. G. Mogilevskaya, A. Y. Zemlyanova, V. I. Kushch, Fiber-and particle-reinforced composite materials with the Gurtin–Murdoch and Steigmann–Ogden surface energy endowed interfaces, *Appl. Mech. Rev.*, **73** (2021), 1–18. https://doi.org/10.1115/1.4051880
9. M. E. Gurtin, A. I. Murdoch, A continuum theory of elastic material surfaces, *Arch. Ration. Mech. Anal.*, **57** (1975), 291–323. https://doi.org/10.1007/BF00261375
10. M. E. Gurtin, A. I. Murdoch, Surface stress in solids, *Int. J. Solids Struct.*, **14** (1978), 431–440. https://doi.org/10.1016/0020-7683(78)90008-2
11. A. I. Murdoch, The propagation of surface waves in bodies with material boundaries, *J. Mech. Phys. Solids*, **24** (1976), 137–146. https://doi.org/10.1016/0022-5096(76)90023-5
12. A. I. Murdoch, The effect of interfacial stress on the propagation of stoneley waves, *J. Sound Vib.*, **50** (1977), 1–11. https://doi.org/10.1016/0022-460X(77)90547-8
13. D. J. Steigmann, R. W. Ogden, Surface waves supported by thin-film/substrate interactions, *IMA J. Appl. Math.*, **72** (2007), 730–747. https://doi.org/10.1093/imamat/hxm018
14. V. A. Eremeyev, G. Rosi, S. Naili, Surface/interfacial anti-plane waves in solids with surface energy, *Mech. Res. Commun.*, **74** (2016), 8–13. https://doi.org/10.1016/j.mechrescom.2016.02.018
15. G. Mikhasev, B. Erbaş, V. A. Eremeyev, Anti-plane shear waves in an elastic strip rigidly attached to an elastic half-space, *Int. J. Eng. Sci.*, **184** (2023), 103809. https://doi.org/10.1016/j.ijengsci.2022.103809
16. S. Dhua, A. Maji, A. Nath, The influence of surface elasticity on shear wave propagation in a cylindrical layer structure with an imperfect interface, *Eur. J. Mech. A. Solids*, **106** (2024), 105318. https://doi.org/10.1016/j.euromechsol.2024.105318
17. F. Jia, Z. Zhang, H. Zhang, X. Q. Feng, B. Gu, Shear horizontal wave dispersion in nanolayers with surface effects and determination of surface elastic constants, *Thin Solid Films*, **645** (2018), 134–138. https://doi.org/10.1016/j.tsf.2017.10.025
18. W. Wu, H. Zhang, F. Jia, X. Yang, H. Liu, W. Yuan, et al., Surface effects on frequency dispersion characteristics of Lamb waves in a nanoplate, *Thin Solid Films*, **697** (2020), 137831. https://doi.org/10.1016/j.tsf.2020.137831
19. D. J. Steigmann, R. W. Ogden, Plane deformations of elastic solids with intrinsic boundary elasticity, *Proc. R. Soc. Ser. A*, **453** (1997), 853–877. https://doi.org/10.1098/rspa.1997.0047
20. D. J. Steigmann, R. W. Ogden, Elastic surface–substrate interactions, *Proc. R. Soc. Ser. A*, **455** (1999), 437–474. https://doi.org/10.1098/rspa.1999.0320
21. V. A. Eremeyev, Strongly anisotropic surface elasticity and antiplane surface waves, *Phil. Trans. R. Soc. A*, **378** (2020), 20190100. https://doi.org/10.1098/rsta.2019.0100
22. C. Rodriguez, Elastic solids with strain-gradient elastic boundary surfaces, *J. Elast.*, **156** (2024), 769–797. https://doi.org/10.1007/s10659-024-10073-w
23. L. Brillouin, *Wave Propagation in Periodic Structures: Electric Filters and Crystal Lattices*, Mcgraw Hill Book Company, New York, 1953. https://doi.org/10.1038/158926a0

24. A. I. Murdoch, Some fundamental aspects of surface modelling, *J. Elast.*, **80** (2005), 33–52. https://doi.org/10.1007/s10659-005-9024-2
25. V. A. Eremeyev, B. L. Sharma, Anti-plane surface waves in media with surface structure: Discrete vs. continuum model, *Int. J. Eng. Sci.*, **143** (2019), 33–38. https://doi.org/10.1016/j.ijengsci.2019.06.007
26. B. L. Sharma, V. A. Eremeyev, Wave transmission across surface interfaces in lattice structures, *Int. J. Eng. Sci.*, **145** (2019), 103173. https://doi.org/10.1016/j.ijengsci.2019.103173
27. J. Achenbach, *Wave Propagation in Elastic Solids*, North Holland, Amsterdam, 1973.
28. G. B. Whitham, *Linear and Nonlinear Waves*, John Wiley & Sons, New York, 1999.
29. E. Barchiesi, M. Laudato, F. Di Cosmo, Wave dispersion in non-linear pantographic beams, *Mech. Res. Commun.*, **94** (2018), 128–132. https://doi.org/10.1016/j.mechrescom.2018.11.002
30. N. Shekarchizadeh, M. Laudato, L. Manzari, B. E. Abali, I. Giorgio, A. M. Bersani, Parameter identification of a second-gradient model for the description of pantographic structures in dynamic regime, *Z. Angew. Math. Phys.*, **72** (2021), 190. https://doi.org/10.1007/s00033-021-01620-9
31. A. Ciallella, I. Giorgio, S. R. Eugster, N. L. Rizzi, F. dell'Isola, Generalized beam model for the analysis of wave propagation with a symmetric pattern of deformation in planar pantographic sheets, *Wave Motion*, **113** (2022), 102986. https://doi.org/10.1016/j.wavemoti.2022.102986
32. R. Fedele, L. Placidi, F. Fabbrocino, A review of inverse problems for generalized elastic media: Formulations, experiments, synthesis, *Continuum Mech. Thermodyn.*, **36** (2024), 1413–1453. https://doi.org/10.1007/s00161-024-01314-3
33. L. Placidi, F. Di Girolamo, R. Fedele, Variational study of a Maxwell-Rayleigh-type finite length model for the preliminary design of a tensegrity chain with a tunable band gap, *Mech. Res. Commun.*, **136** (2024), 104255. https://doi.org/10.1016/j.mechrescom.2024.104255
34. B. L. Sharma, Diffraction of waves on square lattice by semi-infinite rigid constraint, *Wave Motion*, **59** (2015), 52–68. https://doi.org/10.1016/j.wavemoti.2015.07.008
35. B. L. Sharma, On linear waveguides of square and triangular lattice strips: An application of Chebyshev polynomials, *Sādhanā*, **42** (2017), 901–927. https://doi.org/10.1007/s12046-017-0646-4
36. G. I. Mikhasev, V. A. Eremeyev, Effects of interfacial sliding on anti-plane waves in an elastic plate imperfectly attached to an elastic half-space, *Int. J. Eng. Sci.*, **205** (2024), 104158. https://doi.org/10.1016/j.ijengsci.2024.104158
37. G. S. Mishuris, A. B. Movchan, D. Bigoni, Dynamics of a fault steadily propagating within a structural interface, *Multiscale Model. Simul.*, **10** (2012), 936–953. https://doi.org/10.1137/110845732
38. B. Lal Sharma, G. Mishuris, Scattering on a square lattice from a crack with a damage zone, *Proc. R. Soc. A*, **476** (2020), 20190686. https://doi.org/10.1098/rspa.2019.0686
39. B. L. Sharma, Scattering of surface waves by inhomogeneities in crystalline structures, *Proc. R. Soc. A*, **480** (2024), 20230683. https://doi.org/10.1098/rspa.2023.0683
40. M. Brun, A. B. Movchan, N. V. Movchan, Shear polarisation of elastic waves by a structured interface, *Continuum Mech. Thermodyn.*, **22** (2010), 663–677. https://doi.org/10.1007/s00161-010-0143-z

41. G. Rosi, L. Placidi, V. H. Nguyen, S. Naili, Wave propagation across a finite heterogeneous interphase modeled as an interface with material properties, *Mech. Res. Commun.*, **84** (2017), 43–48. https://doi.org/10.1016/j.mechrescom.2017.06.004

42. A. Casalotti, F. D'Annibale, G. Rosi, Optimization of an architected composite with tailored graded properties, *Z. Angew. Math. Phys.*, **75** (2024), 126. https://doi.org/10.1007/s00033-024-02255-2

43. F. dell'Isola, A. Madeo, L. Placidi, Linear plane wave propagation and normal transmission and reflection at discontinuity surfaces in second gradient 3D continua, *ZAMM J. Appl. Math. Mech.*, **92** (2012), 52–71. https://doi.org/10.1002/zamm.201100022

44. L. Placidi, G. Rosi, I. Giorgio, A. Madeo, Reflection and transmission of plane waves at surfaces carrying material properties and embedded in second-gradient materials, *Math. Mech. Solids*, **19** (2014), 555–578. https://doi.org/10.1177/1081286512474016

45. A. Berezovski, I. Giorgio, A. D. Corte, Interfaces in micromorphic materials: Wave transmission and reflection with numerical simulations, *Math. Mech. Solids*, **21** (2016), 37–51. https://doi.org/10.1177/1081286515572244

46. E. Barchiesi, L. Placidi, A review on models for the 3D statics and 2D dynamics of pantographic fabrics, *Adv. Struct. Mater.*, (2017), 239–258. https://doi.org/10.1007/978-981-10-3797-9_14

47. E. Turco, E. Barchiesi, A. Ciallella, F. dell'isola, Nonlinear waves in pantographic beams induced by transverse impulses, *Wave Motion*, **115** (2022), 103064. https://doi.org/10.1016/j.wavemoti.2022.103064

48. S. R. Eugster, Numerical analysis of nonlinear wave propagation in a pantographic sheet, *Math. Mech. Complex Syst.*, **9** (2022), 293–310. https://doi.org/10.2140/memocs.2021.9.293

49. E. Turco, E. Barchiesi, F. dell'Isola, A numerical investigation on impulse-induced nonlinear longitudinal waves in pantographic beams, *Math. Mech. Solids*, **27** (2022), 22–48. https://doi.org/10.1177/10812865211010877

50. V. A. Eremeyev, G. Rosi, S. Naili, On effective surface elastic moduli for microstructured strongly anisotropic coatings, *Int. J. Eng. Sci.*, **204** (2024), 104135. https://doi.org/10.1016/j.ijengsci.2024.104135

AIMS Press

© 2025 the Author(s), licensee AIMS Press. This is an open access article distributed under the terms of the Creative Commons Attribution License (https://creativecommons.org/licenses/by/4.0)